

Chladni Figures Revisited: A Peek Into The Third Dimension

Martin Skrodzki*, Ulrich Reitebuch*, and Konrad Polthier
AG Mathematical Geometry Processing, Freie University Berlin
Arnimallee 6, 14195, Berlin, Germany

{martin.skrodzki,ulrich.reitebuch,konrad.polthier}@fu-berlin.de

Abstract

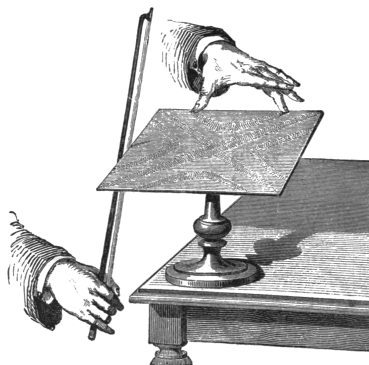
In his 1802 book "Acoustics", Ernst Florens Friedrich Chladni describes how to visualize different vibration modes using sand, a metal plate, and a violin bow. We will review the underlying physical and mathematical formulations and lift them to the third dimension. Finally, we present some of the resulting three dimensional Chladni figures.

Introduction

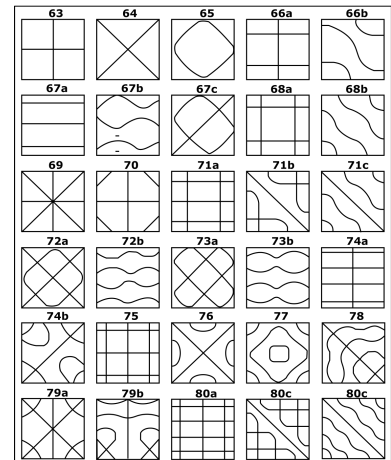
In 1802, Ernst Florens Friedrich Chladni (November 30th, 1756 – April 3rd, 1827, Figure 1a) published his book "Acoustics". The book describes amongst other things an experiment by which different modes of vibration can be visualized. Namely, sand is distributed over a thin metal plate. A violin bow is then struck alongside the plate, causing it to oscillate. See Figure 1b for an illustration. Chladni discovered that the sand grains form different patterns corresponding to the varying vibration modes. His book contains a table of patterns he was able to create in his experiments, see Figure 1c.



(a) Portrait of Ernst Florens Friedrich Chladni by H. Adlard, 19th century.



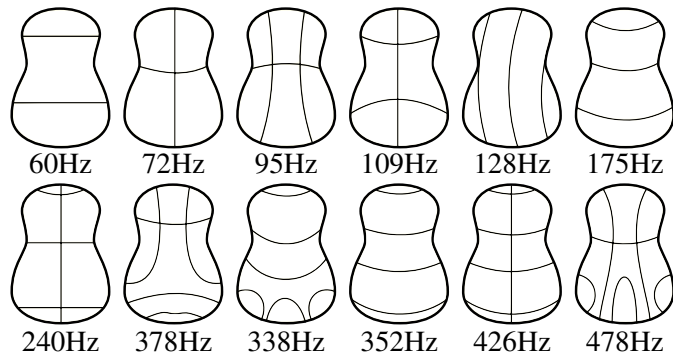
(b) Illustration of the violin bow experiment, taken from [8], 1879.



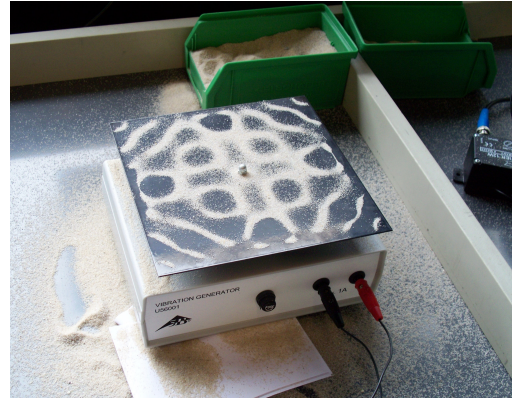
(c) Table of Chladni figures from Chladni's book "Acoustics", 1802.

Figure 1: Historical illustrations of Chladni, his experiments, and results.

Since its first description, the Chladni experiment has been developed further by several other scientists like Margaret Watts-Hughes, Henry Holbrook, or Hans Jenny [2]. Despite their elegance and artistic value, Chladni figures have applications in the construction of musical instruments as illustrated in Figure 2a. Finally, utilizing modern technology such as speakers, the Chladni experiments can easily be recreated with a wide range of frequencies and different thicknesses of metal plates, see Figure 2b.



(a) Chladni figures on the body shape of a guitar, wikimedia commons.



(b) A Chladni figure obtained in a modern experimental setup. ©High Contrast, wikimedia commons.

Figure 2: Application and modern adaption of Chladni figures.

Physical and Mathematical Background

In an experimental physical setup, Chladni figures can be produced by inducing oscillation on some plate. The physical formulation of damped oscillation of a string is given by the following differential equation

$$m \frac{\partial^2}{\partial t^2} h(x, t) + d \frac{\partial}{\partial t} h(x, t) + kh(x, t) = 0, \quad (1)$$

where $h(x, t)$ is the displacement at position x and time t , m is the mass which oscillates, d is the dampening constant, and k is the spring constant. In the following we will always assume $d = 0$ since the physical systems in consideration are all stimulated. Consider the one-dimensional case of an oscillating string. Then equation (1) has two basic solutions, based on the position x on the string and a parameter u

$$\sin(u \cdot \pi \cdot x \pm \sqrt{k/m} \cdot t) \quad \text{and} \quad \cos(u \cdot \pi \cdot x \pm \sqrt{k/m} \cdot t). \quad (2)$$

Chladni figures arise from those linear combinations of (2) which describe a stationary wave. Those are obtained by combining the positive and negative version of (2) such that they can cancel each other out at certain points. Using the trigonometric addition formulas we obtain

$$\sin(u \cdot \pi \cdot x + \sqrt{k/m} \cdot t) + \sin(u \cdot \pi \cdot x - \sqrt{k/m} \cdot t) = 2 \sin(u \cdot \pi \cdot x) \cdot \cos(\sqrt{k/m} \cdot t), \quad (3)$$

with similar results for the difference of the positive and negative formulations, as well as for the \cos terms. When imposing Dirichlet or Neumann boundary conditions on the differential equation,

$$\text{Dirichlet } \left\{ h(0, t) = h(1, t) = 0 \forall t \in \mathbb{R} \quad \text{Neumann } \left\{ \frac{\partial}{\partial x} h(x, t) \Big|_{x=0} = \frac{\partial}{\partial x} h(x, t) \Big|_{x=1} = 0 \forall t \in \mathbb{R} \quad (4)$$

we see from (3) that the boundary conditions can only be satisfied for $u \in \mathbb{Z}$.

Now the \sin -solution from (2) solves the Dirichlet problem from (4) while the \cos -solution from (2) solves the Neumann problem from (4). The corresponding one-dimensional Chladni figure is now given by the zero level set of the following functions, with a parameter $A \in \mathbb{R}$,

$$A \cdot \sin(u \cdot \pi \cdot x) \quad \text{and} \quad A \cdot \cos(u \cdot \pi \cdot x) \quad (5)$$

for the Dirichlet and Neumann problem respectively. Finally, our generalization of Chladni figures to the third dimension uses the following function, with $A, \dots, F \in \mathbb{R}$,

$$\begin{aligned}
 & A \cdot \sin(u \cdot \pi \cdot x) \cdot \sin(v \cdot \pi \cdot y) \cdot \sin(w \cdot \pi \cdot z) + B \cdot \sin(u \cdot \pi \cdot x) \cdot \sin(v \cdot \pi \cdot z) \cdot \sin(w \cdot \pi \cdot y) \\
 & + C \cdot \sin(u \cdot \pi \cdot y) \cdot \sin(v \cdot \pi \cdot x) \cdot \sin(w \cdot \pi \cdot z) + D \cdot \sin(u \cdot \pi \cdot y) \cdot \sin(v \cdot \pi \cdot z) \cdot \sin(w \cdot \pi \cdot x) \quad (6) \\
 & + E \cdot \sin(u \cdot \pi \cdot z) \cdot \sin(v \cdot \pi \cdot x) \cdot \sin(w \cdot \pi \cdot y) + F \cdot \sin(u \cdot \pi \cdot z) \cdot \sin(v \cdot \pi \cdot y) \cdot \sin(w \cdot \pi \cdot x),
 \end{aligned}$$

respectively with cos terms for the Neumann boundary conditions. Note that similar to the one-dimensional case, conditions (4) hold if and only if $u, v, w \in \mathbb{Z}$. These generalizations follow in a manner similar to the one described above from (1) when inserting three positions x, y , and z . For a more thorough account on the physics behind Chladni figures see [6] and for a description of the underlying mathematics refer to [4].

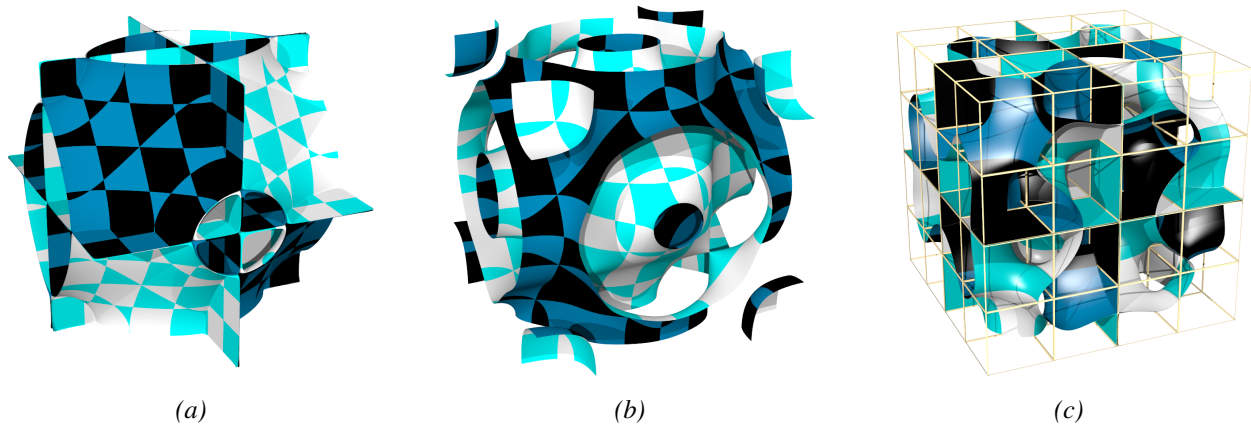


Figure 3: Figures (a) and (b) are dual to each other as the parameters are the same and only the sin are replaced by cos for the second picture, while (c) displays the cubical grid creating the checkerboard pattern on front- and backside. Note that the grid is twice as fine in all other figures.

Image Production Techniques

Apart from physical experiments, as shown in Figure 2b, computer experiments are conducted in order to produce Chladni figures. A well-written description for the production of Chladni figures with MATLAB is given in [3], where the authors employ both a spectral and finite difference method. A different route is taken by [1], where the Chladni figures are the result of a stochastic process. Finally, [7] uses Max/Msp/Jitter to create images of three-dimensional Chladni figures.

Our approach consists of plotting the zero level set of the expression given in (6) in the bounding box $[-1, 1]^3$ for prescribed parameters A, \dots, F and u, v, w by utilizing PovRay [5]. For colored versions of the images we refer the interested reader to the online version of this article. Parameters for the Chladni figures shown in Figures 3 and 4 are given in the table below. Note that these shown patterns could be experimentally reproduced and thus confirmed, e.g. by placing some light particles in viscose fluid which is stimulated by a speaker.

Figure 3c shows the front side (light colors) and back side (dark colors) as well as the coarse cubical grid that induces a checkerboard pattern on each side of the surface by using different colors for each two neighboring cubical cells. The grid is chosen twice as fine in Figures 3a, 3b, and 4.

Figure	Type	u	v	w	A	B	C	D	E	F
3a	sin	1.0	1.0	2.0	0.5	2.0	2.0	1.5	1.5	0.5
3b	cos	1.0	1.0	2.0	0.5	2.0	2.0	1.5	1.5	0.5
3c	sin	3.0	1.0	2.0	0.2	2.0	2.0	0.2	0.2	2.0
4a	sin	2.0	4.0	1.0	1.0	1.0	1.0	1.0	1.0	1.0
4b	cos	2.0	4.0	1.0	1.0	1.0	1.0	1.0	1.0	1.0
4c	sin	2.0	4.0	1.0	1.0	1.0	1.0	1.0	1.0	1.0
4d	sin	2.0	3.0	1.0	0.5	-0.5	2.0	1.5	1.5	-1.1
4e	sin	4.0	1.0	2.0	0.2	2.0	2.0	0.2	0.2	2.0
4f	cos	1.0	0.0	-2.0	-1.0	1.8	1.8	-1.0	-1.0	1.8

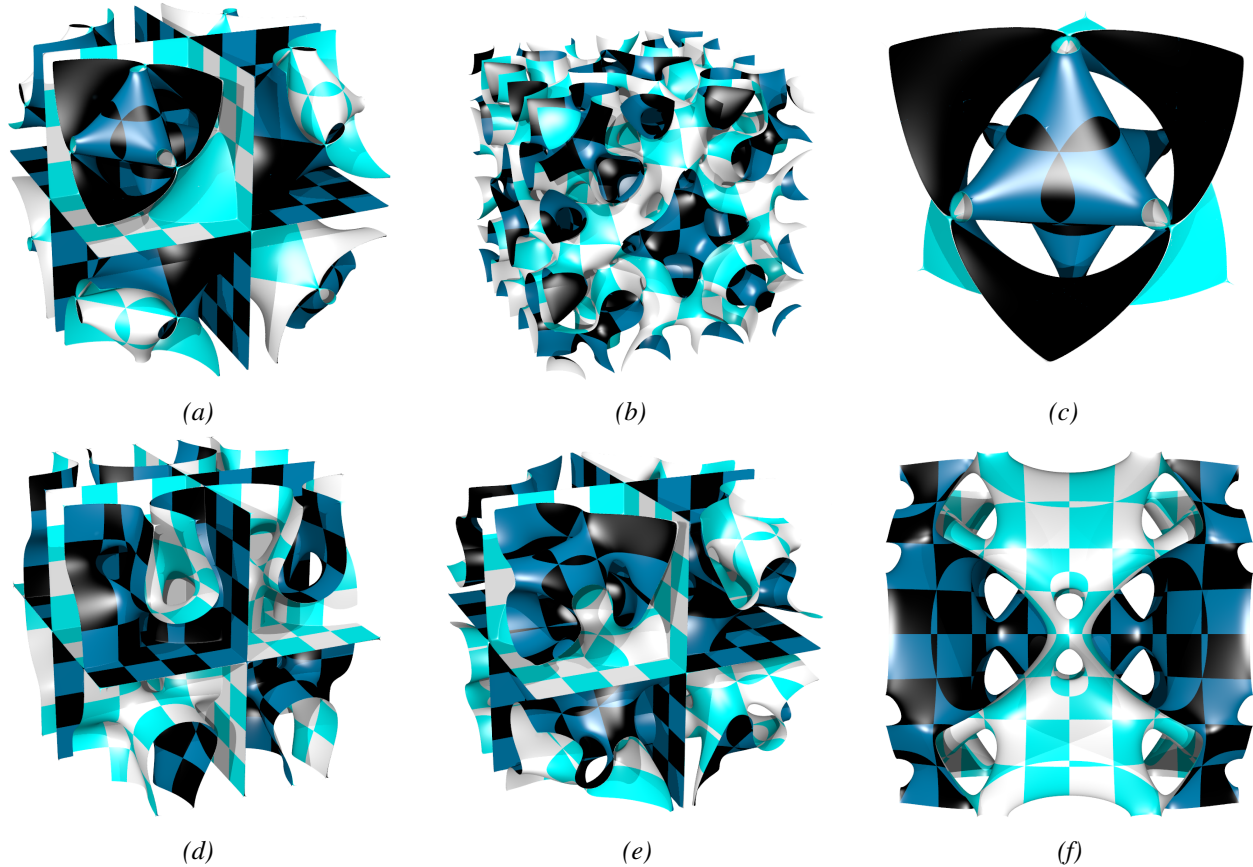


Figure 4: Figure (c) is a detail of (a) as it only shows the level set in $[0, 1]^3$. Note that (f) does not have a dual since $v = 0$ would result in the whole expression (6) being zero.

Acknowledgments This work is supported by the Einstein Center for Mathematics Berlin and the Berlin Mathematical School as well as the SFB Transregio 109: Discretization in Geometry and Dynamics.

References

- [1] Jaime Arango and Carlos Reyes. Stochastic models for chladni figures. *Proceedings of the Edinburgh Mathematical Society*, pages 1–14, 2015.
- [2] Frank Findeiß. Die Entdeckung der Chladnischen Klangfiguren. Ursprünge und Weiterentwicklung im historischen Kontext. *Leuphana Universität Lüneburg, Germany*, 2015.
- [3] Martin J. Gander and Felix Kwok. Chladni figures and the tacoma bridge: motivating pde eigenvalue problems via vibrating plates. *SIAM Review*, 54(3):573–596, 2012.
- [4] Bruno Lévy and Hao Richard Zhang. Spectral mesh processing. In *ACM SIGGRAPH 2010 Courses*, page 8. ACM, 2010.
- [5] Persistence of Vision Pty. Ltd. Raytracer (version 3.7). [http://http://www.povray.org/](http://www.povray.org/). Accessed: 2016-04-19.
- [6] Herbert John Pain. *The physics of vibrations and waves*. John Wiley, 2005.
- [7] Oscar Sol. 3d chladni patterns. <https://www.flickr.com/photos/oscarsol/sets/72157641551929843>. Accessed: 2016-03-15.
- [8] William Henry Stone. *Elementary Lessons on Sound*. Macmillan & Company, 1879.